Analysis of the Influence of Number of Segments on Similarity Level in Wound Image Segmentation Using K-Means Clustering Algorithm

Furizal [1,*], Syifa'ah Setya Mawarni [2], Son Ali Akbar [3], Anton Yudhana [4], Murinto Kusno [5]
[1,2] Master Program of Informatics, Universitas Ahmad Dahlan, Yogyakarta, Indonesia
[3,4] Department of Electrical Engineering, Universitas Ahmad Dahlan, Yogyakarta, Indonesia
[5] Department of Informatics, Universitas Ahmad Dahlan, Yogyakarta, Indonesia
Email: [1] furizal.id@gmail.com, [2] syifa.mawarni19@gmail.com, [3] sonali@ee.uad.ac.id, [4] eyudhana@ee.uad.ac.id, [5] murintokusno@tif.uad.ac.id
*Corresponding Author

***Abstract*— This study underscores the importance of wound image segmentation in the medical world to speed up first aid for victims and increase the efficiency of medical personnel in providing appropriate treatment. Although the body has a protective function from external threats, the skin can be easily damaged and cause injuries that require rapid detection and treatment. This study used the K-Means clustering algorithm to segment the external wound image dataset consisting of three types of wounds, namely abrasion, puncture, and laceration. The results showed that K-Means clustering is an effective method for segmenting wound images. The greater the number of segments used, the better the quality of the resulting segmentation. However, it is necessary to take into account the specific characteristics of each type of wound and the number of segments used in order to choose the most suitable segmentation method. Evaluation using various metrics, such as VOI, GCE, MSE, and PSNR, provides an objective assessment of the quality of segmentation. The results showed that abrasion wounds were easier to segment compared to puncture wounds and lacerations. In addition, the size of the image file also affects the speed of program execution, although it is not always absolute depending on the characteristics of the image.**

Keywords*—*Image segmentation, K-Means, Wound imagery, Image Processing

I. INTRODUCTION

The body has a protective function from various external threats, but skin tissue is easily damaged and causes injury. Skin vulnerability presents various types of injuries including animal or human bites, accidental injuries, sharp or blunt objects, temperature and radiation [1]. Wound is damage to the protective function of the skin accompanied by loss of epithelial tissue continuity with or without damage to other tissues such as muscles, bones, and nerves caused by several factors, namely pressure, incisions, and surgical injuries [2].

External wounds have three levels of severity, namely level 1 (superficial), level 2 (superficial partial-thickness), and level 3 (full thickness). Wound segmentation can provide a clear picture of how serious the wound is by looking at the color depth. The deeper the color, the worse and higher the severity of the wound.

Object detection is an identification process. Generally, identification is carried out using a camera as an object capturer and then the image obtained is further identified.

According to the Central Statistics Agency, there were around 272 injuries due to natural disasters and fires in 2019-2021 in Jakarta. Object recognition or object detection on wounds can help speed up the process of first aid to victims and increase the efficiency of medical personnel in providing handlers to victims.

Object detection using segmentation has been widely done in the medical world, such as Riska Nanda et al segmenting medical images on Fibroa Adenoma Mammae (FAM) objects or benign tumors in the breast using the Sobel algorithm [3]. The image used by FAM ultrasound results is in .dcom format with Matlab R2009a as its tool. The results of segmentation of medical images with sobel algorithms are good for determining edges on FAM objects, but images with less resolution of edge detection are difficult. In addition to breasts, image segmentation with Deep Learning on lung image segmentation by Muhammad Hussein produced the best value using the U-Net EfficientNetb0 algorithm with a dice value of 0.967 and a jaccard of 0.937 but for the speed of time the MobileNet U-net algorithm [4]. The dataset used was X-Ray images with a total of 80 normal lung images and 58 others had abnormalities. Other research on segmentation with lung objects has also been conducted by Sintha Syaputri and Zulkarnain using Active Contour algorithm and Matlab R2015a as their tools [5]. The result of this study is that Active Contour can segment well depending on the parameter value.

Medical image segmentation has a variety of algorithms that can be used, one of which is K-Means clustering. K-Means is an unsupervised learning algorithm for solving clustering problems in a faster time than C-Means Fuzzy [6]. Segmentation on medical images using the K-Means algorithm has been carried out by R. S. D. Wijaya et al [7] and Dwiza Riana et al [8] on cervical cancer objects and W. M. Baihaqi et al on leukocyte nucleus segmentation [9].

Medical image segmentation is centered on vital objects, even though the skin is the outermost layer or shield for the body, so there is rarely segmentation using wound objects. External wound segmentation helps wound treatment be

faster and more precise. Identification of wounds becomes clearer so that appropriate treatment is given.

Research contribution to analyzing external wound image segmentation using k-means clustering and the effect of the number of segments on external wound image segmentation.

II. METHOD

This study began with the collection of wound image datasets. The dataset that has been obtained will be processed at the preprocessing stage such as resizing, cropping, noise correction, and converting color images to grayish images. Once preprocessing is complete, the new grayish image will be segmented using the K-means Clustering method. The research flow can be seen in Fig 1.

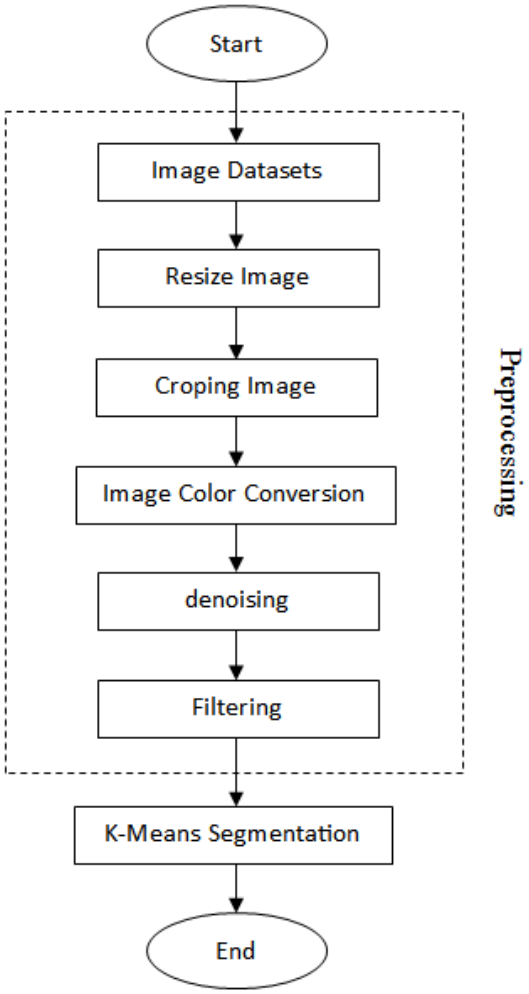

Fig. 1. Research flow

A. Image Dataset

The image data used is external wound image data. The image dataset was taken from Kaggle with a total of nine data consisting of three classes, namely abrasion wounds, lacerations, and puncture wounds. Each class has three image data. The external wound image dataset is a dataset that is quite difficult to find. the hospital did not allow external wound datasets to be collected. dataset was taken from Kaggle, which is one of the platforms that provides external wound image datasets.

B. Preprocessing

1) Image Resize

The image data obtained is not in the same size. In order for the segmentation process to work optimally, it takes an image resizing process or resizing images with the aim of equalizing the size of each image. The study resized each image to 640x640 pixels. This size is at the medium point, not too tight and not too loose so that the segmentation process becomes more efficient but the image of the wound is still clearly visible.

2) Image Color Conversion

The original image has a red, green, and blue color base which is often also called RGB image. RGB images have a total pixel intensity value of 24-bits, each color channel has an 8-bit pixel intensity value which means it has a color variation of 28 = 256 color degrees (0 to 255). A grayscale image is a grayscale image with an intensity value of at most 255 in white to black with an intensity value of at least 0 [10]. Image conversion from RGB images to grayscale images aims to simplify images so that the segmentation process becomes more efficient.

3) Noise Repair

Genuine imagery is usually contaminated with noise, whether it's during image shooting, image delivery, image downloading. Noise is a disturbance caused by the storage of digital data received by image data receivers that can interfere with image quality [11]. The use of noise and filters is based on measuring image quality values. There are four image quality measurements, namely Mean Square Error (MSE) [12]-[13], Peak Signal Noise Ratio (PSNR) [14]-[16], Variation of Information (VOI) [17]-[18], and Global Consistency Error (GCE) [19]-[21]. The smaller the MSE value, the better the recovery value from the noise effect, and in PSNR the higher the value, the better because it is considered close to the original image.

a) Mean Square Error (MSE) and Peak Signal Noise Ratio (PSNR)

MSE and PSNR are expressed mathematically using Equations 1 and 2.

$$MSE = \frac{1}{m \times n} \sum_{i=0}^{m} \sum_{j=0}^{n} [f'(i,j) - (f(i,j)]^2 \quad (1)$$

$$PSNR = 10\, log_{10} \left(\frac{Max}{\sqrt{MSE}} \right) \quad (2)$$

Where m and n are the column and row sizes of the image, f (I,j) is the original image and f' (I,j) is the recovered image. Max is the maximum possible pixel value, if 8 Bits means 28-1 = 255.

b) Variation of Information (VOI) and Global Consistency Error (GCE)

VOI or information variation serves to measure the amount of missing information obtained between two clusters, while GCE or global consistency error according to D. Martin is some error measure to measure consistency between human partitions and algorithm partitions. VOI and GCE are mathematically expressed using equations 3 and 4.

$$VOI\,(FSx, FSy) = E\,(FSx) + E\,(FSy) - 2M\,(FSx, FSy) \quad (3)$$

Where FSx and FSy exhibit K-Means segmentation, entropy is represented by E(FS), then E(FSx, FSy) indicates a combination of two images, and M (FSx, FSy) sends reciprocal information from the two images.

$$\text{GCE}\ (S_x, S_y) = \frac{1}{m}\min\left(\sum_j E(S_x, S_y, p_i), \left(\sum_j E(S_y, S_{yx}, p_i\right)\right) \quad (4)$$

Where S_x and S_y show two segmentations and pi represents the position of the pixel.

Based on these measurements, the closest thing to the original image is using uniform noise with a 3x3 Median low-pass filter. Produces clear images with minimal noise contamination so that segmentation becomes more effective.

C. K-Means Segmentation

The K-Means clustering algorithm is a centroid model. The centroid model is a model that uses centroids to create clusters, centroid is the midpoint value of a cluster and centroid is used to calculate the distance of an object to the centroid. A data object is included in a cluster if it has the shortest distance to the cluster centroid.

The K-means algorithm uses an iterative process to obtain a cluster database. It takes the desired initial number of clusters as input and produces the final centroid point as output. The K-means method will choose k patterns as the starting point of the centroid randomly. K-means uses the parameters in equation 5.

$$\bar{v}_{ij} = \frac{1}{N}\sum_{k=0}^{N_i} x_{kj} \quad (4)$$

V_{ij} is the centroid/average of the first cluster for the j variable, N_i is the amount of data that is a member of the i cluster, i,k is the index of the cluster, j is the index of the variable, xkj is the k data value in the cluster for the j variable.

III. Results and Discussion

In the results of this discussion, wound images were segmented using the K-Means algorithm by testing nine different wound images. This wound image is divided into three types of wounds, namely abrasion, puncture, and laser wounds. All images used have jpg extension. This test aims to test the extent of the ability of the K-Means algorithm to segment the three types of wound images used as test data. This segmentation was tested in three test categories, namely image segmentation with 2 segments, 3 segments, and 4 segments. The selection to test three different numbers of segments, namely 2, 3, and 4, in testing K-Means segmentation algorithm is aimed at exploring how well the algorithm can adapt to various levels of complexity in wound images. By including different numbers of segments, we can evaluate the algorithm's performance in scenarios with few objects (2 segments), moderate complexity (3 segments), or higher complexity (4 segments). This helps us understand whether the algorithm exhibits strong generalization capabilities across different situations and ensures that the segmentation results can be optimized according to different task contexts. The original image and segmented image can be seen in Table 1.

Table 1 displays the original image and segmented images that have been processed using the K-Means algorithm. The original image is the image before the segmentation process, while the segmented image is the image that has been processed to divide the pixels by color. Every color image consists of a combination of colors formed from the pixels in the image, creating a complete image. There are several color models commonly used in image processing, such as the RGB color model that uses red, green, and blue color channels, the CMYK color model used in printing, the HSB color model that describes the shades, saturation, and brightness of colors, and the CIE-XYZ color model used in lighting science and industry. Based on the original image used along with the RGB color distribution outlined in 3D graphics as in Fig. 2.

When viewed with the naked eye, the results of new scar segmentation will be more clearly visible when the image is segmented into 4-segments. While results on 2-segments tend to show less than optimal results, because some wounds are not detected properly. Dark skin is always identified as a wound. In addition, blood splashes on uninjured skin are also identified as wounds by the results of 2-segment segmentation. However, to better see the extent of the performance of the K-Means algorithm in segmenting images, it is based on four indicators, namely the value of VOI, GCE, MSE, and PSNR. The values of these four indicators can be seen in full in Table 2.

Table 2 provides complete information regarding image segmentation that has been carried out by providing VOI, GCE, MSE, and PSNR values. In addition, it also calculates the program execution time during image processing. The file size of each image is also displayed to see its influence in the image process. The effect of file size on program execution time is shown in Fig. 3.

Fig. 3 indicates that the image file size greatly affects the ET of the program. However, this statement is not absolute because there are some files that are higher in size, but programs can execute faster when compared to lower file sizes. For example, the 3rd abrasion wound image has a lower file size when compared to the 1st and 2nd laser wound images. But the required ET is greater. The highest ET was obtained in the 2nd abrasion wound image of the 4-segment, with an ET of 2.0206 s. While the lowest ET was obtained in the 2nd puncture wound image of the 2-segment, with an ET of 0.0653 s.

In addition, Fig. 3 also shows how the number of image segments affects ET. The more segments used, the slower the program execution. In this test, images divided into 4-segments require more ET when compared to 2-segments and 3-segments. Although this is also not absolute, the tests carried out show almost certainty. Because only 2 tests contradict this statement, namely ET 2nd puncture wound image with 3-segment (0.1936 s) greater than ET at 4-segment (0.1922 s) and ET 3rd puncture wound image with 3-segment (0.5314 s) greater than ET at 4-segment (0.5214 s).

Then, in determining the difference in information, the percentage of inconsistent pixels, the average square difference between pixel intensity, and the comparison between peak signal power in the original image and distortion power in the segmented image, the VOI, GCE, MSE, and PSNR values depicted in Fig 4.

Table 1. Wound image segmentation results

No	Types of Wounds		Original Image	Segmentation Results		
				2 Segments	3 Segments	4 Segments
1	Abrasion	1		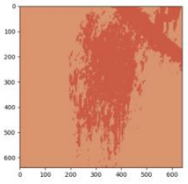	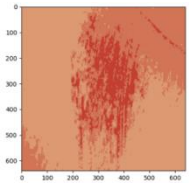	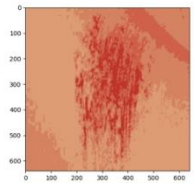
		2		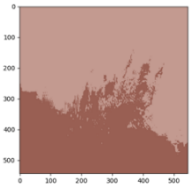	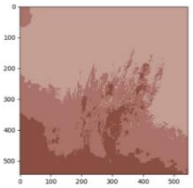	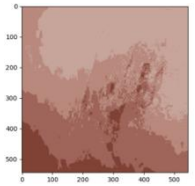
		3		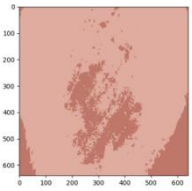	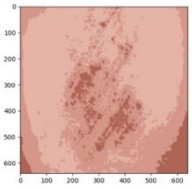	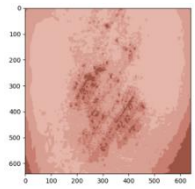
2	Stab	1		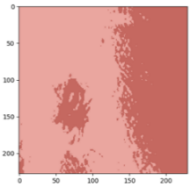	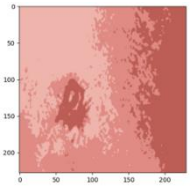	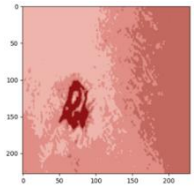
		2		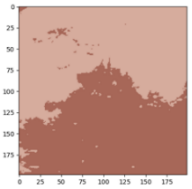	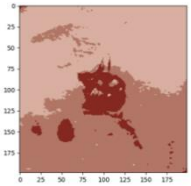	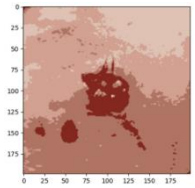
		3		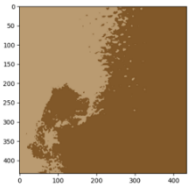	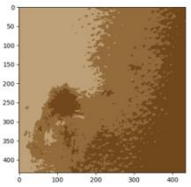	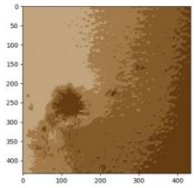
3	Laser	1		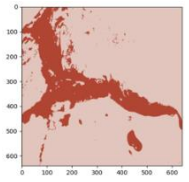	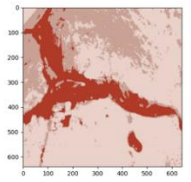	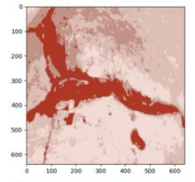
		2		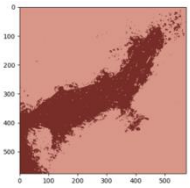	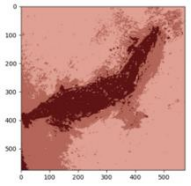	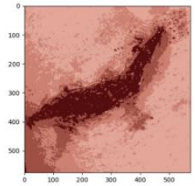
		3		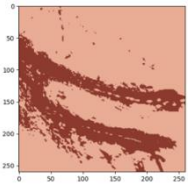	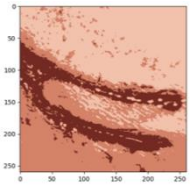	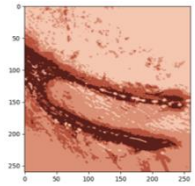

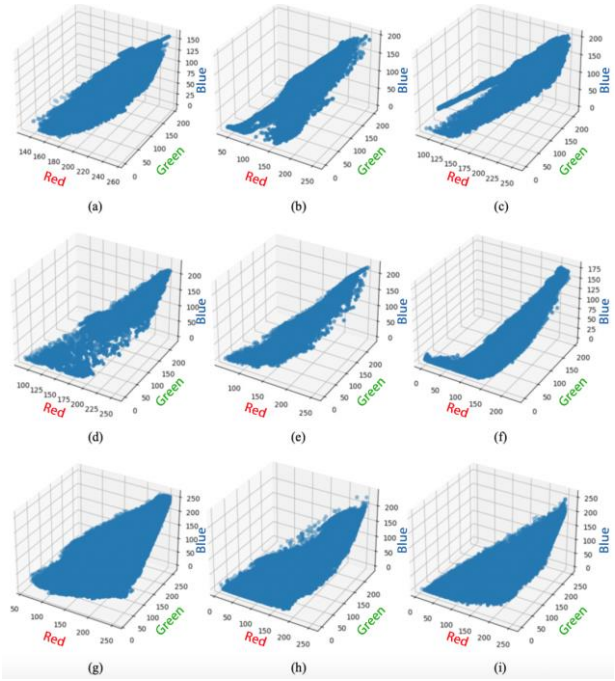

Fig. 2. RGB color distribution 3D graphic (a) First image of abrasion wound, (b) The second image of the abrasion wound, (c) The third image of the abrasion wound, (d) The first image of the stab wound, (e) The image of both stab wounds, (f) The image of the three stab wounds, (g) First image of laser wound, (h) Images of both laser wounds, (i) Image of the three laser wounds

Table 2. Wound image segmentation results

No	Types of Wounds	Original Image		2-Segments					3-Segments					4-Segments				
		Imagery to-	File size (KB)	VOI	GCE	MSE	PSNR	ET	VOI	GCE	MSE	PSNR	ET	VOI	GCE	MSE	PSNR	ET
1	Abrasion	1	138	6.3218	0.9712	207.21	24.967	0.6873	6.0785	0.9613	114.41	27.546	0.9599	5.8753	0.9571	83.353	28.922	1.6309
		2	121	7.0982	0.9795	289.05	23.521	0.4026	6.9543	0.9726	178.15	25.623	0.7555	6.7307	0.9612	117.99	27.412	1.2398
		3	140	6.8201	0.9746	263.45	23.924	0.7553	6.621	0.9687	155.89	26.203	1.0154	6.5326	0.9631	110.64	27.692	2.0206
2	Stab	1	50	7.1391	0.977	423.51	21.862	0.1052	6.988	0.9738	270.34	23.812	0.1595	6.8136	0.9696	159.16	26.112	0.1656
		2	42	7.381	0.9769	534.6	20.851	0.0653	7.1679	0.9692	248.18	24.183	0.1936	6.9836	0.9694	168.91	25.854	0.1922
		3	112	7.3688	0.9792	398.88	22.122	0.2992	7.0344	0.9774	228.79	24.537	0.5314	6.6558	0.9693	151.04	26.34	0.5214
3	Laser	1	239	7.9809	0.9842	664.89	19.903	0.8723	7.4285	0.9811	360.78	22.558	0.8219	7.4377	0.9703	263.23	23.927	1.2572
		2	258	7.7414	0.9852	722.26	19.544	0.7508	7.3257	0.9796	366.46	22.491	0.6773	7.3184	0.9754	254.32	24.077	0.9817
		3	89	7.9178	0.99	981.04	18.214	0.1492	7.476	0.9784	453.45	21.566	0.1678	7.3754	0.9755	291.63	23.483	0.2588

Fig. 4a is the VOI value in each image segmentation. This VOI result shows that the more the number of segments, the lower the potential VOI value. This means that the more the number of segments, the degree of similarity between the original image and the better the image of the segment results and vice versa. Then to get the percentage of pixels that are inconsistent between the segmented image and the original image, Fig. 4b explains that the more the number of segments, the more potential to produce a lower GCE value. This proves that the more the number of segments, the more potential for consistency of the two images.

On Fig. 4c, MSE describes the average squared difference between the pixel intensity in the segmented image and the original image. The lower the value, the more similar the two images are. Just like GCE, MSE also shows the same results. The more the number of segments, the more potential to produce a lower MSE value. This proves that the more the number of segments, the more similar the two images.

Meanwhile, to get a comparison between the peak signal power in the original image with the distortion power in the segmented image, the PSNR value is needed as in Fig. 4d. The highest average PSNR value is obtained from segmentation of abrasion wound images. While the lowest average PSNR value is obtained from segmentation of laser wound images. The higher the value, the more similar the two images are. This means that the original image of the abrasion wound can be better segmented by K-Means than the image of the puncture wound and laser. This is also supported by VOI, GCE, and MSE values in each image segmentation.

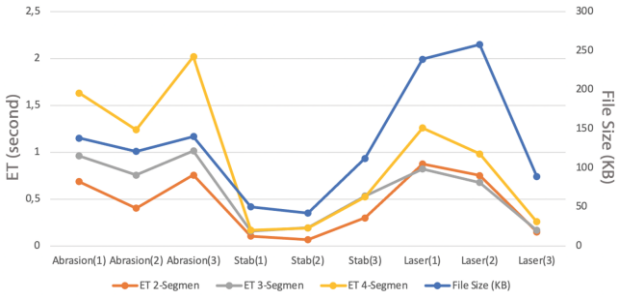

Fig. 3. Impact of file size on ET

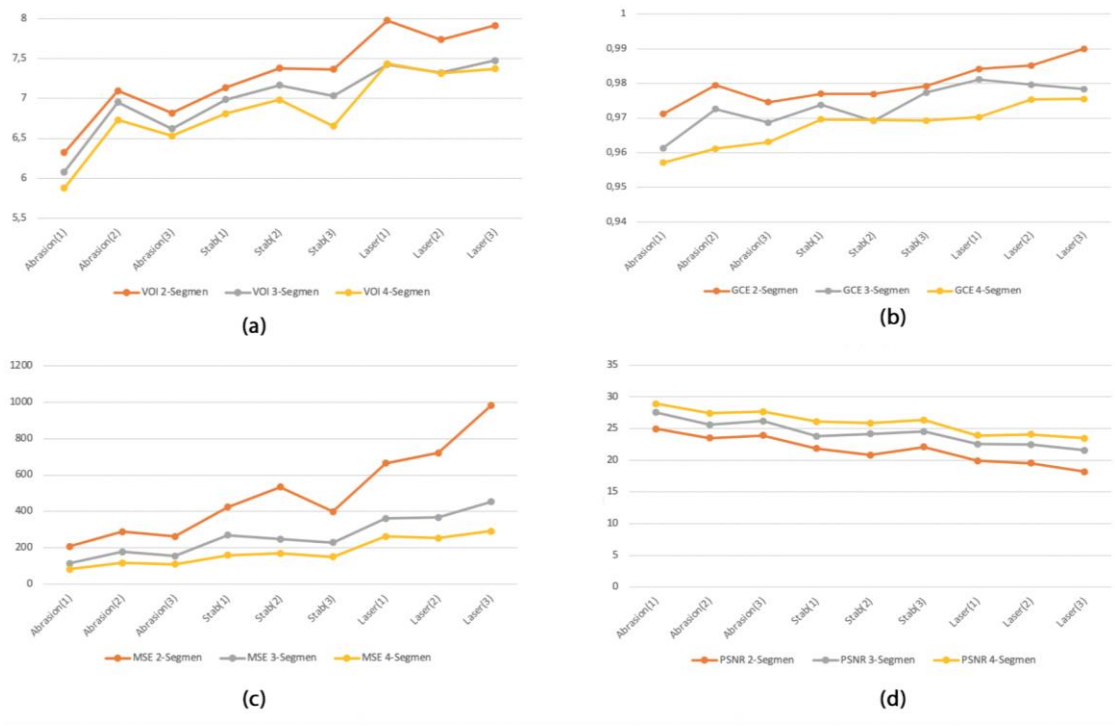

Fig. 4. (a) VOI value; (b) GCE value; (c) MSE value; and (d) the PSNR value of each image segmentation

IV. CONCLUSION

The use of the K-Means algorithm in segmenting wound images through testing on three types of wounds (abrasion, puncture, and laser) with variations in the number of segments showed mixed results. Segmentation with a larger number of segments tends to produce better results in terms of similarity and consistency between the segmented image and the original image. Evaluation using evaluation metrics such as VOI, GCE, MSE, and PSNR provides an objective assessment of segmentation quality, with abrasion wound imagery generally providing better results. However, it is necessary to pay attention to the characteristics of each type of wound and the number of segments in choosing the appropriate method of segmentation. These conclusions provide important insights in the development of image segmentation techniques for medical and analytical applications. The results of this study need to be investigated further to provide maximum results in wound image segmentation. It is recommended to explore optimal preprocessing techniques, develop hybrid methods that combine multiple segmentation algorithms, and involve external evaluation with better ground truth to obtain accurate validation and a better understanding of segmentation quality. In addition, the development of clinical applications using wound image segmentation is also an important step to test its usefulness and effectiveness in medical practice.

REFERENCES

[1] G. Zaman Khan *et al*., "An Efficient Deep Learning Model based Diagnosis System for Lung Cancer Disease," *2023 4th International Conference on Computing, Mathematics and Engineering Technologies (iCoMET)*, pp. 1-6, 2023, https://doi.org/10.1109/iCoMET57998.2023.10099357.

[2] C. N. Elangwe, S. N. Morozkina, R. O. Olekhnovich, A. Krasichkov, V. O. Polyakova, and M. V. Uspenskaya, "A Review on Chitosan and Cellulose Hydrogels for Wound Dressings," *Polymers (Basel)*, vol. 14, no. 23, p. 5163, 2022, https://doi.org/10.3390/polym14235163.

[3] P. Cho, H. J. Yoon, "Evaluation of U-net-based image segmentation model to digital mammography," *Medical Imaging 2021: Image Processing*, vol. 11596, pp. 593-599, 2021, https://doi.org/10.1117/12.2581401.

[4] M. M. Hasan, M. Md. Jahangir Kabir, M. R. Haque and M. Ahmed, "A Combined Approach Using Image Processing and Deep Learning to Detect Pneumonia from Chest X-Ray Image," *2019 3rd International Conference on Electrical, Computer & Telecommunication Engineering (ICECTE)*, pp. 89-92, 2019, https://doi.org/10.1109/ICECTE48615.2019.9303543.

[5] E. Jangam, A. C. S. Rao, "Segmentation of lungs from chest X rays using firefly optimized fuzzy C-means and level set algorithm," *International Conference on Recent Trends in Image Processing and Pattern Recognition*, pp. 303-311, 2019, https://doi.org/10.1007/978-981-13-9184-2_27.

[6] C. Zhang *et al*., "White Blood Cell Segmentation by Color-Space-Based K-Means Clustering," *Sensors*, vol. 14, no. 9, pp. 16128–16147, 2014, https://doi.org/10.3390/s140916128.

[7] C. Sun *et al*., "Gastric histopathology image segmentation using a hierarchical conditional random field," *Biocybernetics and Biomedical Engineering*, vol. 40, no. 4, pp. 1535-1555, 2020, https://doi.org/10.1016/j.bbe.2020.09.008.

[8] D. Riana, S. Hadianti, S. Rahayu, Frieyadie, M. Hasan, I. N. Karimah, R. Pratama, "Repomedunm: A new dataset for feature extraction and training of deep learning network for classification of pap smear images," *International Conference on Neural Information Processing*, pp. 317-325, 2021, https://doi.org/10.1007/978-3-030-92307-5_37.

[9] W. M. Baihaqi, C. R. A. Widiawati, T. Insani, "K-Means Clustering Based on Otsu Thresholding For Nucleus of White Blood Cells Segmentation," *Jurnal RESTI (Rekayasa Sistem dan Teknologi Informasi)*, vol. 4, no. 5, pp. 907-914, 2020, https://doi.org/10.29207/resti.v4i5.2309.

[10] K. Liu, W. Wang, and J. Wang, "Pedestrian Detection with Lidar Point Clouds Based on Single Template Matching," *Electronics*, vol. 8, no. 7, p. 780, 2019, http://dx.doi.org/10.3390/electronics8070780.

[11] B. Karthik, T. K. Kumar, S. P. Vijayaragavan, M. Sriram, "Removal of high density salt and pepper noise in color image through modified cascaded filter," *Journal of Ambient Intelligence and Humanized Computing*, vol. 12, pp. 3901-3908, 2021, https://doi.org/10.1007/s12652-020-01737-1.

[12] U. Sara, M. Akter, and M. S. Uddin, "Image Quality Assessment through FSIM, SSIM, MSE and PSNR—A Comparative Study,"

Journal of Computer and Communications, vol. 7, no. 3, pp. 8-18, 2019, https://doi.org/10.4236/jcc.2019.73002.

[13] T. Badriyah, N. Sakinah, I. Syarif, and D. R. Syarif, "Segmentation Stroke Objects based on CT Scan Image using Thresholding Method," *2019 First International Conference on Smart Technology & Urban Development (STUD)*, pp. 1–6. 2019, https://doi.org/10.1109/STUD49732.2019.9018825.

[14] A. R. W. Putri, "Classification of Breast Cancer Using the Digital Mammogram Method," *JATISI (Jurnal Teknik Informatika dan Sistem Informasi)*, vol. 9, no. 4, pp. 2752–2761, 2022, https://doi.org/10.35957/jatisi.v9i2.2100.

[15] C. Huang, X. Li, and Y. Wen, "AN OTSU image segmentation based on fruitfly optimization algorithm," *Alexandria Engineering Journal*, vol. 60, no. 1, pp. 183–188, 2021, https://doi.org/10.1016/j.aej.2020.06.054.

[16] H. Jia, X. Peng, W. Song, C. Lang, Z. Xing, and K. Sun, "Multiverse Optimization Algorithm Based on Lévy Flight Improvement for Multithreshold Color Image Segmentation," *IEEE Access*, vol. 7, pp. 32805-32844, 2019, https://doi.org/10.1109/ACCESS.2019.2903345.

[17] L. Guo, P. Shi, L. Chen, C. Chen, and W. Ding, "Pixel and region level information fusion in membership regularized fuzzy clustering for image segmentation," *Information Fusion*, vol. 92, pp. 479–497, 2023, https://doi.org/10.1016/j.inffus.2022.12.008.

[18] B. Jai Shankar, K. Murugan, A. Obulesu, S. Finney Daniel Shadrach, and R. Anitha, "MRI Image Segmentation Using Bat Optimization Algorithm with Fuzzy C Means (BOA-FCM) Clustering," *J Med Imaging Health Inform*, vol. 11, no. 3, pp. 661–666, 2021, https://doi.org/10.1166/jmihi.2021.3365.

[19] D. Anandan, S. Hariharan, and R. Sasikumar, "Deep learning based two-fold segmentation model for liver tumor detection," *Journal of Intelligent & Fuzzy Systems*, vol. 45, no. 1, pp. 77–92, 2023, https://doi.org/10.3233/JIFS-230694.

[20] M. Poojary and Y. Srinivas, "Optimization Technique Based Approach for Image Segmentation," *Curr Med Imaging Rev*, vol. 19, no. 10, 2023, https://doi.org/10.2174/1573405619666221104161441.

[21] H. Liu, X. Diao, and H. Guo, "Quantitative analysis for image segmentation by granular computing clustering from the view of set," *J Algorithm Comput Technol*, vol. 13, p. 174830181983305, 2019, https://doi.org/10.1177/1748301819833050.